Int. J. Cancer: **120,** 978–984 (2006)

FAST TRACK

Sensitivity of magnetic resonance imaging of dendritic cells for *in vivo* tracking of cellular cancer vaccines

Pauline Verdijk[1], Tom W.J. Scheenen[2], W. Joost Lesterhuis[3], Giulio Gambarota[2], Andor A. Veltien[2], Piotr Walczak[5], Nicole M. Scharenborg[1], Jeff W.M. Bulte[5], Cornelis J.A. Punt[3], Arend Heerschap[2], Carl G. Figdor[1] and I. Jolanda M. de Vries[1,4]*

[1]*Department of Tumorimmunology, Nijmegen Centre for Molecular Life Science, Radboud University Nijmegen Medical Centre, Nijmegen, The Netherlands*
[2]*Department of Radiology, Nijmegen Centre for Molecular Life Science, Radboud University Nijmegen Medical Centre, Nijmegen, The Netherlands*
[3]*Department of Medical Oncology, Nijmegen Centre for Molecular Life Science, Radboud University Nijmegen Medical Centre, Nijmegen, The Netherlands*
[4]*Department of Pediatric Oncology, Nijmegen Centre for Molecular Life Science, Radboud University Nijmegen Medical Centre, Nijmegen, The Netherlands*
[5]*The Russell H. Morgan Department of Radiology and Radiological Science, Division of MR Research, and Institute for Cell Engineering, John Hopkins University School of Medicine, Baltimore, MD, USA*

Success of immunotherapy with dendritic cells (DC) to treat cancer is highly dependent on their interaction with and activation of antigen specific T cells. To maximize DC–T cell contact accurate delivery of the therapeutic cells into the lymph node, or efficient trafficking of DC to the lymph nodes of the patient is essential. Since responses are seen in some patients but not in others, monitoring of the injected cells may be of major importance. Tracking of cells with magnetic resonance (MR) imaging is a non-invasive method that provides detailed anatomical information and is therefore more informative for the evaluation of the localization of therapeutic cells after injection than *e.g.* scintigraphic imaging. To challenge the sensitivity of this novel technique, we investigated the minimum amount of label and the number of cells required for MR imaging and the effect of labeling on DC function. DC were labeled with different concentrations of a clinically approved MR contrast agent consisting of superparamagnetic iron oxide particles and were imaged at both 3 and 7 T. Our results demonstrate the following: (*i*) When loaded with 30 (±4) pg Fe/cell, cell numbers as low as 1,000 cells/mm^3 at 3 T and 500 cells/mm^3 at 7 T could be readily imaged; (*ii*) Labeling does not affect cell viability and function; (*iii*) Because of its high spatial resolution and sensitivity, MRI is ideally suited to track therapeutic cells *in vivo*.

Key words: magnetice resonance imaging; dendritic cell vaccine; superparamagnetic iron oxide; cellular therapy; cell tracking; sensitivity

Dendritic cells (DC) are professional antigen presenting cells that can be exploited to induce antitumor responses in cancer patients. Although vaccination of patients with autologous DC loaded with tumor antigens is still in its infancy, clinical effectiveness has been shown in several patients.[1,2] Since responses are seen in some patients and not in others, monitoring of the injected cells may be important. Previously, radioactive labels like ^{111}Indium-oxinate have been used to track DC after vaccination.[3–6] Radionuclide labeling allows an estimation of the percentage of cells that have migrated from the injection site to potential immunoreactive sites, but provides no information on the exact location of the cells within the anatomical context. Also, due to the short half-life of the radionuclide, long-term tracking is limited and the radiation of the injected DC may theoretically have adverse effects on the surrounding cells. Therefore, labeling of cells with contrast agents for magnetic resonance (MR) imaging may be an attractive alternative, since with the added anatomical information a more detailed visualization of the distribution of injected cells can be obtained. For MR-based tracking of injected cells labeling with superparamagnetic iron oxide (SPIO) particles is currently explored.[7] Different cell types have been loaded with SPIO either directly or with the use of transfection agents[8] or other coatings, however, most studies are constricted to animal models[9–15] and *in vitro* experiments.[12,16,17]

Human stem cells have been labeled with SPIO with or without the aid of transfection agents,[18–24] while monocytes[11,16] and the human macrophage cell line THP-1[17] efficiently phagocytose SPIO. Only limited data is available on the minimum iron content per cell that is necessary for detection by MR imaging. Cell labeling efficiencies vary from 0.8 to 50 pg of Fe/cell; however, Daldrup-Link *et al.*[20] showed that for MR imaging of labeled cells at 1.5 T a Fe concentration of ca. 2.6 pg/cell is minimally required. Moreover, little is known about the number and the density of cells that is needed for imaging the SPIO-labeled cells against the background, after they have been injected into patients or animals. *In vivo* tracking of SPIO-labeled cells has been limited to proof of principle experiments in mice and rat. Either cells were injected locally in one specified location and local migration was imaged over time,[11,18,25] or large numbers of magnetically labeled cells were injected intravenously in mouse tumor models and accumulation of injected cells at the tumor was demonstrated.[10,12,22,23] Kircher *et al.* estimated to be able to detect densities of SPIO-labeled cells of approximately 10^3 cells/mm^3 in live mice.[10] In mouse brains—which have a high homogeny and low signal intensity in GRE images—100–500 labeled cells can be imaged at high magnetic fields strengths (17.5 and 7 T).[26,27] Heyn *et al.* recently demonstrated single cell detection of SPIO-labeled cells in the brain of mice, but further development of methods and hardware are needed before this can be performed in humans.[28] Recently, we showed comparable sensitivities in humans in a first clinical study with human monocyte-derived DC labeled with SPIO and imaged *in vivo* on a 3 T MR whole body scanner.[29] In this report we explored the minimal concentration of Fe/cell and the lowest amount of cells that is needed for detection with MRI on 3 and 7 T by labeling human DC with increasing concentrations of SPIO.

Grant sponsor: Dutch Cancer Society; Grant numbers: KUN 1999/1950, 2004/3126; Grant sponsors: The Netherlands Organization for Scientific Research, the TIL-foundation, and NOTK-foundation; Grant number: 920-03-250; Grant sponsor: NIH; Grant number: RO1 NS045062.
***Correspondence to:** NCMLS, Radboud University Nijmegen Medical Centre, P.O. Box 9101, 6500 HB Nijmegen, the Netherlands.
Fax: +31-24-3540339. E-mail: j.devries@ncmls.ru.nl
Received 15 June 2006; Accepted after revision 30 August 2006
DOI 10.1002/ijc.22385
Published online 12 December 2006 in Wiley InterScience (www.interscience.wiley.com).

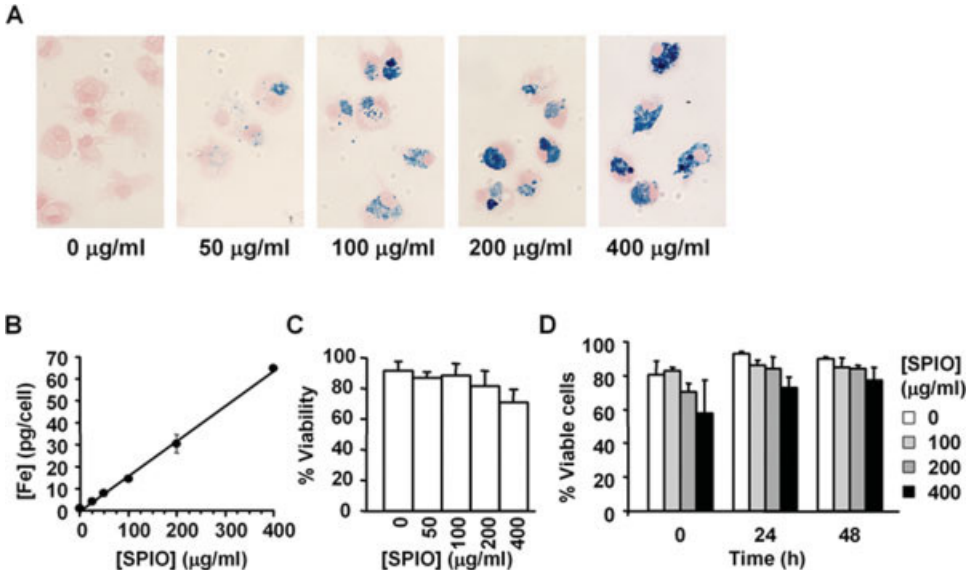

FIGURE 1 – SPIO-labeling of DC. At day 3 after monocyte isolation SPIO was added to the cells in different concentrations ranging from 0 to 400 (g/ml). The amount of iron that was present in the mature DC at the end of the culture was visualized with Prussian Blue staining (A) and measured with a Ferrozin-based spectrophotometric iron assay (B). (*a*) Prussian Blue staining of cytospins showing the iron distribution for DC cultured with different concentrations of SPIO. (*b*) Mean concentration of Fe per cell after culturing with SPIO. The graph represents the mean of 4 independent experiments. Error bars represent standard error of the mean. (*c*) Viability of mature DC and SPIO–DC determined by trypan blue exclusion. The graph represents the mean of 4–11 independent experiments. Error bars represent the standard deviation. (*d*) Viability of mature DC and SPIO–DC after prolonged culture determined by trypan blue exclusion. The graph represents the mean of 3 experiments. Error bars represent the standard deviation. [Color figure can be viewed in the online issue, which is available at www.interscience.wiley.com.]

Furthermore, we determined the optimal concentration of Fe/cell and estimate the density of cells that will be detectable *in vivo* in a heterogeneous background. In addition, we show that DC function is not compromised by labeling with SPIO.

Material and methods

DC culture and labeling

DC were generated from adherent peripheral blood mononuclear cells (PBMC) by culturing in the presence of interleukin-4 (500 U/ml) and granulocyte-monocyte colony stimulating factor (800 U/ml) (both Cellgenix, Freiburg, Germany). For SPIO-labeling, DC were cultured with different concentrations of SPIO ranging from 0 to 400 μg ferrumoxide/ml (Endorem®, Laboratoire Guerbet, Aulnay-sous-Bois, France), which was added 3 days after the onset of DC culturing. At day 5, DC were matured with autologous monocyte-conditioned medium supplemented with prostaglandin E_2 (10 μg/ml, Pharmacia & Upjohn, Puurs, Belgium) and 10 ng/ml recombinant tumor necrosis factor-α (Cellgenix, Freiburg, Germany) for 48 hr, as described previously.[30,31] Labeling of mature DC with ^{111}In-oxine in 0.1 M Tris-HCl (pH 7.0) for 15 min at room temperature[3,30] resulted in 100 μCi activity per 7.5×10^6 cells. Cells were washed 3 times with phosphate buffered solution. Radiolabeling efficiency was determined by measuring activity in both the cell pellet and the washing buffer. Iron labeling efficiency was verified by Prussian Blue staining. Total iron content of SPIO-labeled DC (SPIO–DC) was assessed by a Ferrozin-based spectrophotometric assay following acid-digestion of labeled cell samples.[18,32,33] The iron content per cell was calculated for each cell concentration and expressed as the average +/− SD. Cell viability was determined by Trypan Blue staining. For vaccination, DC were pulsed with the melanoma peptides gp100:154–162, gp100:280–288, tyrosinase:369–376[3] and labeled with ^{111}In-oxinate.

Flow cytometry

Fluorescence activated cell sorter (FACS) analysis was performed using a Becton Dickinson FACSCalibur. The following fluorochrome-conjugated monoclonal antibodies were used: anti-HLA class I (W6/32), anti-HLA DR/DP (Q5/13), anti-CD80 (all Becton Dickinson, Mountain View, California), anti-CD83 (Beckman Coulter, Mijdrecht, The Netherlands), anti-CD86 (Pharmingen, San Diego, CA), and anti-Chemokine Receptor 7 (kind gift of Martin Lipp).

T-cell stimulation

The allostimulatory capacity of SPIO–DC was tested in a mixed lymphocyte reaction (MLR). Allogeneic T cells were cocultured with DC or SPIO–DC in a 96-well tissue culture microplate. After 4 days of culture, 1 μCi/well of tritiated thymidine was added for 8 hr, and incorporation of tritiated thymidine was measured in a beta-counter.

Peptide specific T-cell stimulatory capacity was tested by coculturing DC or SPIO–DC that were loaded with the gp100:154–162 peptide or an irrelevant peptide with a gp100:154–162 specific T-cell line (DC:T ratio 1:5).[34] After 48 hr the cytokines in the supernatant were analyzed with a cytometric bead array for human Th1/Th2 cytokines (BD Biosciences, San Diego, CA). Cellular responses against the protein keyhole limpet hemocyanin (KLH) were measured in a proliferation assay. Briefly, PBMC isolated from blood samples taken after 3 biweekly DC vaccinations, were plated in a 96-well tissue culture microplate with autologous DC that were cultured with or without KLH and with or without SPIO. After 4 days of culture, 1 μCi/well of tritiated thymidine was added for 8 hr, and incorporation of tritiated thymidine was measured in a beta-counter.

Migration assay

Flat-bottomed plates (96-well; Costar, Corning, NY) were coated with 20 μg/ml fibronectin (Roche, Mannheim, Germany) and blocked with 0.01% gelatin (Sigma Chemical Co., St. Louis, MO). We used our previously established migration assay to study migration of DC.[35] Four thousand DC (50 μl) per well were seeded on fibronectin-coated plates, resulting in 100 cells per image. DC were recorded for up to 60 min, after which, migration

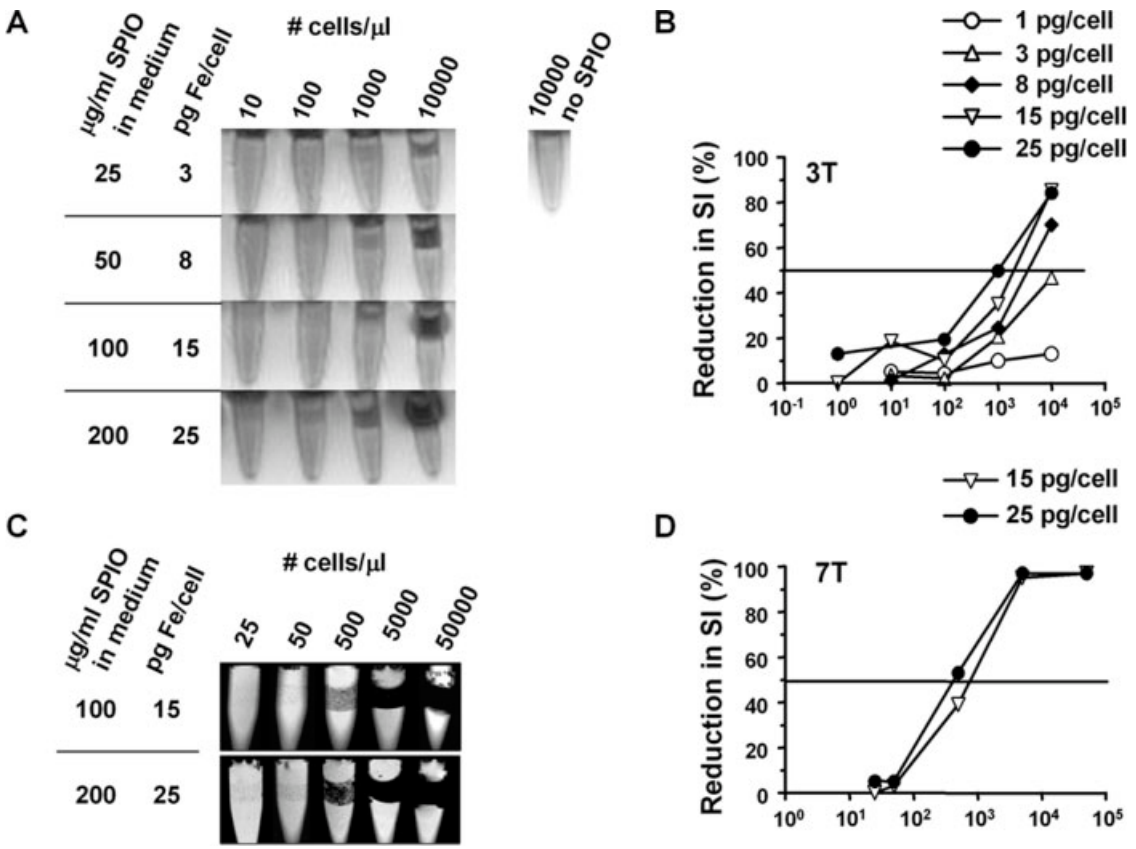

FIGURE 2 – Magnetic resonance imaging of gelatin embedded SPIO–DC on a 3 T whole body scanner (*a*) and a 7 T MR system (*b*). DC were labeled with increasing amounts of SPIO and embedded in 6% gelatin in different cell densities in between 2 layers of 8% gelatin. (*a*) GRE images of SPIO–DC in different concentrations at 3 T. (*b*) GRE images of SPIO–DC in different concentrations at 7 T. [(*c*), (*d*)] Reduction in signal intensity (SI) caused by the presence of SPIO–DC in the cell-layer as a percentage of the signal intensity of a control area of similar size at 3 T (*c*) and 7 T (*d*).

tracks of individual DC were analyzed. The velocity is defined as the speed during time intervals in which the cell has actually relocated.

MR imaging

MR imaging was performed on a 3 T whole body MR system (Siemens Magnetom Trio, Erlangen, Germany) with a matrix of surface array coils for signal reception and a 7 T MR-system with horizontal bore (Surrey Medical Imaging Systems, Surrey, United Kingdom) with a 20 mm diameter radiofrequency coil. Varying numbers of DC (10^2–10^6) were embedded in 100 µl of 6% gelatin in between 2 layers of 8% gelatin in PBS in a 250 µl eppendorf tube. Samples were imaged using a T2*-weighted gradient echo (GRE) pulse sequence at 3 T (repetition time (TR) 800 ms, mean echo time (TE) of 3 combined echoes 15 ms, flip angle 35°; resolution 0.5 × 0.5 × 5.5 mm^3), and at 7 T (TR_c = 1,500 ms and TE = 9 ms; resolution 0.115 × 0.115 × 1.0 mm^3).

Results

SPIO particles are efficiently taken up by monocyte-derived DC

DC efficiently endocytosed the SPIO particles as visualized by Prussian Blue staining (Fig. 1*a*). Significant loss of cell viability and yield by SPIO was detected only at high concentrations (400 µg/ml) of SPIO, where circa 50% of the cells were recovered after maturation. Quantitative spectrophotometrical analysis showed that there was an almost linear correlation (r = 0.98) between the uptake of cellular SPIO and the concentration of the nanoparticles in the culture medium (Fig. 1*b*). At 200 µg/ml SPIO iron uptake was optimal with >99% of the cells containing iron with an average of 30 pg Fe/cell without compromising cell viability (Fig. 1*c*). When SPIO–DC were harvested, washed and cultured for two more days in the absence of SPIO and maturation factors, viability of the cells was comparable to unlabeled DC (Fig. 1*d*) and yield was only compromised for DC labeled with 400 µg/ml of SPIO (data not shown).

In vitro detection threshold of SPIO-DC

To explore the detection threshold of the SPIO-labeled cells on 3 and 7 T MR scanners, we labeled DC with concentrations of SPIO ranging from 0 to 200 µg/ml. Different concentrations of SPIO–DC were embedded in gelatin (to mimic distribution of DC in tissue) and imaged both on a 3 T (Fig. 2*a*) and on a 7 T MR-scanner (Fig. 2*b*). As expected, the level of the SPIO-induced decrease in signal intensity was in both cases dependent on the concentration of iron oxide per cell and the concentration of SPIO–DC. For each sample the ratio of the signal intensity in the cell containing gel over the signal intensity of cell free gel was calculated as a measure for the level of signal intensity decrease due to SPIO (Figs. 2*c* and 2*d*). At an iron concentration of 25 pg/cell (200 µg/ml SPIO/ml culture medium) a significant decrease in signal intensity was still distinguishable at 100 cells/mm^3 at 3 T and at 50 cells/mm^3 at 7 T (Figs. 2*a* and 2*b*). As the MR signal intensity of tissues is higher and more heterogeneous than that of the *in vitro* test samples we expect that *in vivo* a 50% signal decrease in a GRE image will still be detectable. When cells were loaded with 25 pg Fe/cell a 50% decrease in signal intensity was obtained at a cell concentration of 10^3 cells/mm^3 on the 3 T MR system. However, at 3 pg Fe/cell the 50% decrease in signal intensity was not yet reached at 10^4 cells/mm^3 (Fig. 2*c*). Thus, sensitivity of MR

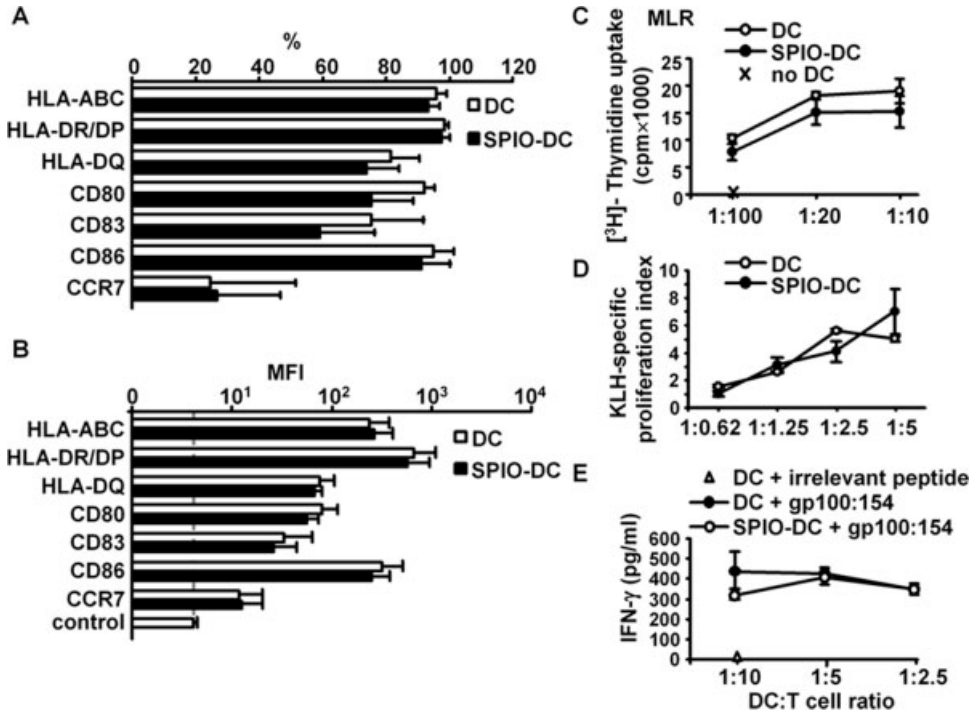

Figure 3 – Addition of SPIO during DC culture does not affect maturation or T-cell activation. [(*a*), (*b*)] Flowcytometric analysis of expression of HLA-DR/DP, CD80, CD86, CD83 and CCR7 on DC cultured with or without 200 μg/ml SPIO from day 3 until day 7. The percentage of marker positive cells (%, A) and the average mean fluorescent intensity (MFI, B) are depicted ($n = 4$), error bars represent the standard deviation. (*c*) Mixed lymphocyte reaction of DC and SPIO-DC with PBMC of allogeneic donor. The graph shows the counts per minute after [3H]-thymidine incorporation and is representative for 4 experiments. Error bars show the standard deviation. (*d*) KLH-specific memory T-cell proliferation. DC and SPIO-DC that were loaded with or without KLH were cocultured with autologous PBMC. The graph shows the proliferation index and is representative for 4 experiments. Error bars show the standard deviation. (*e*) Interferon-γ production of T-cells stimulated with DC cultured with or without SPIO, loaded with or without relevant peptides.

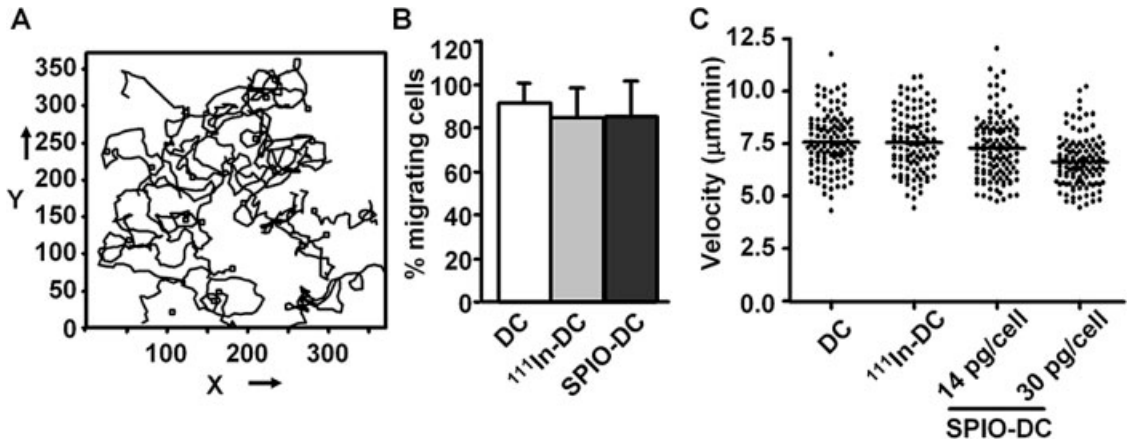

Figure 4 – Effect of ^{111}Indium- or SPIO-labeling on DC migration on fibronectin. (*a*) Example of the traversed path of DC migrating on fibronectin in 1 hr. The x and y axis represent the coordinates of the imaged field in μm. (*b*) Percentage of migrated DC of both SPIO- or ^{111}In-labeled and unlabeled DC. Error bars show the standard deviation. (*c*) Velocity of unlabeled DC, DC labeled with ^{111}In or labeled with 100 or 200 μg/ml of SPIO in culture medium, resulting in ca. 14 and 30 pg Fe/cell. Data points represent the velocity of individual cells; horizontal bars indicate the mean velocity (mean ± standard deviation: DC: 7.6 ± 1.3 μm/min; DC + ^{111}In: 7.5 ± 1.4 μm/min; SPIO-DC 14 pg Fe/cell: 7.2 ± 1.5 μm/min; SPIO-DC 30 pg Fe/cell: 6.6 ± 1.2 μm/min). Data are representatives of 3 experiments.

imaging for SPIO-labeled cells depends on both cell density and on iron concentration per cell.

Labeling of DC with SPIO does not influence surface marker expression and T cell stimulatory capacity in vitro

Because the threshold of detection of labeled DC with MRI depended on the amount of Fe/cell, and cell viability was affected above a concentration of 200 μg/ml SPIO/ml, we selected this concentration for cell tracking with MR imaging *in vivo*. As SPIO particles were present during 4 days of the DC culture, SPIO particles may affect the maturation of the DC and their function. Phenotypic characterization of the cells revealed that the percentages of DC and SPIO–DC expressing surface markers associated with DC maturation were comparable (Fig. 3*a*), and that both unlabeled and SPIO-labeled cells expressed similar levels of these markers (Fig. 3*b*).

The capacity of SPIO-labeled cells to process and present antigen and to stimulate T-cells was tested in the following assays: (*i*) non-specific T-cell stimulation in a MLR, (*ii*) antigen uptake, processing and presentation, assessed by antigen-specific proliferation (*iii*) antigen-specific activation of CD8 T cells measured by the production of IFN-γ. In MLRs SPIO-labeling of the DC had no effect on the induction of T cell proliferation in 2 out of 4 experiments and in 2 experiments proliferation was slightly reduced (example in Fig. 3*c*). This indicated that SPIO-labeling had little to no effect on alloresponses. Secondly, we compared the capacity of unlabeled DC and SPIO–DC to take up, process and present protein antigens. In our vaccination studies, KLH is added to the immature DC culture as a tool for immunological monitoring of the patients. As SPIO-particles are added simultaneously with KLH, antigen presentation may be affected by the contrast fluid. The mature DC that had been cultured with KLH and/or SPIO-particles were then cocultured with PBMC from patients with known KLH reactive T-cells.[36] Although counts were lower with SPIO–DC both with and without the addition of KLH than with unlabeled cells, the antigen-specific proliferation indices were similar for DC and SPIO–DC (Fig. 3*d*). In the third assay, the effect of SPIO-labeling of DC on the activation of antigen-specific CD8 T cells was analyzed by coculturing labeled and unlabeled cells loaded with gp100:154–162 peptide with a gp100:154–162-specific T cell line.[34] Secretion of IFN-γ was determined as a measure of CD8 T-cell activation. Labeled and unlabeled cells were equally able to activate T cells as both induced similar amounts of peptide-specific production of IFN-γ as unlabeled cells (Fig. 3*e*). In addition, levels of other cytokines, such as IL-4, IL-5 and IL-10 were all below the detection limit for all conditions. These results not only indicate that T cell stimulatory capacity is not affected by SPIO-labeling, but also that antigen-processing and presentation is not changed.

Effect of SPIO-labeling on DC migration

For efficient *in vivo* stimulation of T cells it is essential that injected DC migrate from the injection site to the lymph nodes and into the T cell zones. To determine the migratory capacity of SPIO–DC, random migration on the extracellular matrix protein fibronectin[35] was studied and compared with unlabeled DC and DC labeled with ^{111}In. The tracks of the DC were followed with live microscopy and their traversed paths were analyzed (example is shown in Fig. 4*a*). No significant differences were detected in the number of migrating DC (Fig. 4*b*). Under all labeling conditions DC migration was efficient. However, with increasing amounts of iron oxide the velocity of the SPIO–DC was slightly decreased (Fig. 4*c*).

Discussion

Correct delivery and targeting of cellular vaccines is crucial for the success of cell-based therapies. Tracking cells with MRI is a non-invasive and safe method that provides detailed information on the anatomical location of the therapeutic cells. We established the sensitivity of detection of SPIO-labeled DC with MRI by determining the minimal amount of iron per cell and the minimal cell density that is required to distinguish the labeled DC from the background. With 25 pg Fe/cell we estimate to detect 1,000 cells/mm^3 with a 3 T whole body MR scanner in patients treated with SPIO-labeled therapeutic cells.

The SPIO-compound Endorem® was used in these studies as it is an attractive contrast agent for monitoring cell migration. It is biodegradable and the only FDA-approved SPIO that is currently applicable in the clinic. Endorem® (Europe; Feridex® in USA) is an established agent for liver MR imaging[37] and has been studied as a cell tracking agent both *in vitro* and in animal models. Because immature DC are highly phagocytic they efficiently phagocytosed Endorem®, like monocytes and THP-1 cells,[11,16,17] without the need for extra handling of the cells or the use of transfection agents, which is desirable for use in clinical studies. The amount of iron oxide phagocytosed by human monocyte-derived DC increased linearly with the concentration of SPIO in the culture medium. MR imaging of these SPIO-labeled DC demonstrated that the effect on the signal intensity in T2*-weighted MRI depends on both the concentration of iron oxide per cell and the cell density. Cell densities of 100 cells/mm^3 in GRE images of *in vitro* samples could be imaged using a 3 T whole body scanner under clinically applicable settings. However, the background signal of the phantom setup for the *in vitro* experiments is homogenous and lacks tissue-dependent variation in signal intensity. As we are interested in tracking DC to lymph node regions that have a high tissue diversity and large variations in tissue-dependent signal intensities, we estimate that *in vivo* a 50% signal decrease in a GRE image will be detectable. By using this threshold to compensate for conditions *in vivo* and the signal to noise ratio, we calculated that local accumulations of approximately 10^3 DC/mm^3 will be detectable. As the *in vivo* spatial resolution is typically $0.5 \times 0.5 \times 3.5$ mm^3 (= voxel size) this means we can detect 0.9×10^3 DC/voxel, provided that several adjacent voxels are positive. When the Fe concentration/cell is less, the sensitivity of detecting those cells decreases accordingly. These results demonstrate the importance of improving labeling efficacy for different therapeutic cells for MR tracking after transplantation *in vivo*.

One way to enhance the sensitivity of MRI for SPIO-labeled cells is to increase the magnetic field strength. For example, after resection, patient material can be imaged at 7 T experimental MR systems to evaluate the presence and location of SPIO-labeled cells without the need to destruct the tissue by sectioning. At the same time, the first 7 T whole body scanners are now becoming available for the scientific community, and in the long run for clinical practice. We imaged SPIO-labeled DC with our 7 T experimental MR system using sequences comparable to clinical settings in order to estimate the sensitivity of these scanners. We demonstrate that SPIO–DC can be imaged in cell densities as low as 50 cells/mm^3. By calculating the 50% signal intensity decrease we estimate to be able to detect at least 500 cells/mm^3 in *ex vivo* tissues, representing a concentration of 7 cell/voxel at a resolution of $0.12 \times 0.12 \times 1.0$ mm^3. Again, the sensitivity decreased proportionally with decreasing concentrations of intracellular SPIO. At a dose of 400 μg SPIO/ml dendritic cell viability was strongly decreased. Therefore, we selected the highest dose of SPIO (200 μg/ml) at which cells were still viable to test the effect of SPIO on cell phenotype and function. SPIO-labeling did not interfere with DC maturation, antigen presentation and T cell activation, which has also been described for bone marrow derived DC in mice.[38] *In vitro* migration of SPIO–DC was still intact, although the velocity of the cells was somewhat lower, probably due to the extra cargo of the cells and physical hindrance caused by the high amount of SPIO-containing vesicles in the cell. The capacity to migrate was also evident after intranodal vaccination as SPIO-labeled cells were found in the T cell areas of both the injected LN and subsequent nodes.[29]

As yet, immunomonitoring of cellular immunotherapies has proven difficult, as the immune responses are often weak or local. We showed that the effect of DC vaccinations can be monitored using a delayed type hypersensitivity reaction.[39] The route by which the DC vaccine is administered may play a significant role in the efficacy of the DC vaccine. The optimal administration route is still under investigation.[6,40,41] Using MR tracking, delivery and trafficking of cellular vaccines can be readily monitored, facilitating the evaluation of different vaccination strategies. Recently, we demonstrated that human monocyte-derived DC labeled with SPIO can be effectively imaged on a 3 T MR whole body scanner after intranodal injection into melanoma patients.[29] Due to its spatial resolution the number of lymph nodes positive for DC from the vaccine could be determined more accurately than with scintigraphic imaging. More importantly, with MR imaging we could assess whether delivery of SPIO-labeled cells

into the lymph node was accurate. We observed that in 50% of the patients DC were not correctly injected into the LN, which could not be perceived with scintigraphic imaging. As correct delivery and targeting is crucial for the efficacy of cellular therapies, this demonstrates the importance of accurate imaging of cellular vaccines after injection into the patient in the evaluation of cellular therapies that are in the experimental phase. To improve efficacy of cellular vaccines it will be necessary to study the homing of the therapeutic cells in detail. From the data presented here, we conclude that with 3 T MRI whole body scanners local accumulations of >1,000 SPIO-labeled cells can be detected when the iron concentration is at least 25 pg Fe/cell or more. In the evolving field of NMR imaging and spectroscopy improved scanners and data handling will lead to higher resolutions. In combination with the development of MR whole body scanners with higher magnetic fields this more detailed tracking of labeled therapeutic cells will be enabled.

Acknowledgements

Ing. Mary-lène Brouwer, Ing. Mandy van de Rakt, Ing. Annemiek de Boer, Dr. Sandra Croockewit, Dr. Mariëlle Philippens, Dr. Simon Strijk, Ing. Emile Koenders, Dr. Peter Laverman, Dr. Frank Preijers, Dr. Otto Boerman, Ing. Paul Ruijs are acknowledged for their assistance.

References

1. Banchereau J, Palucka AK. Dendritic cells as therapeutic vaccines against cancer. Nat Rev Immunol 2005;5:296–306.
2. Lesterhuis WJ, de Vries IJ, Adema GJ, Punt CJ. Dendritic cell-based vaccines in cancer immunotherapy: an update on clinical and immunological results. Ann Oncol 2004;15 (Suppl 4):iv145–iv151.
3. de Vries IJ, Krooshoop DJ, Scharenborg NM, Lesterhuis WJ, Diepstra JH, van Muijen GN, Strijk SP, Ruers TJ, Boerman OC, Oyen WJ, Adema GJ, Punt CJ, et al. Effective migration of antigen-pulsed dendritic cells to lymph nodes in melanoma patients is determined by their maturation state. Cancer Res 2003;63:12–17.
4. Morse MA, Coleman RE, Akabani G, Niehaus N, Coleman D, Lyerly HK. Migration of human dendritic cells after injection in patients with metastatic malignancies. Cancer Res 1999;59:56–8.
5. Mackensen A, Krause T, Blum U, Uhrmeister P, Mertelsmann R, Lindemann A. Homing of intravenously and intralymphatically injected human dendritic cells generated in vitro from CD34+ hematopoietic progenitor cells. Cancer Immunol Immunother 1999;48:118–22.
6. Ridolfi R, Riccobon A, Galassi R, Giorgetti G, Petrini M, Fiammenghi L, Stefanelli M, Ridolfi L, Moretti A, Migliori G, Fiorentini G. Evaluation of in vivo labelled dendritic cell migration in cancer patients. J Transl Med 2004;2:27.
7. Modo M, Hoehn M, Bulte JW. Cellular MR imaging. Mol Imaging 2005;4:143–64.
8. Frank JA, Miller BR, Arbab AS, Zywicke HA, Jordan EK, Lewis BK, Bryant LH, Jr, Bulte JW. Clinically applicable labeling of mammalian and stem cells by combining superparamagnetic iron oxides and transfection agents. Radiology 2003;228:480–7.
9. Arbab AS, Jordan EK, Wilson LB, Yocum GT, Lewis BK, Frank JA. In vivo trafficking and targeted delivery of magnetically labeled stem cells. Hum Gene Ther 2004;15:351–60.
10. Kircher MF, Allport JR, Graves EE, Love V, Josephson L, Lichtman AH, Weissleder R. In vivo high resolution three-dimensional imaging of antigen-specific cytotoxic T-lymphocyte trafficking to tumors. Cancer Res 2003;63:6838–46.
11. Zelivyanskaya ML, Nelson JA, Poluektova L, Uberti M, Mellon M, Gendelman HE, Boska MD. Tracking superparamagnetic iron oxide labeled monocytes in brain by high-field magnetic resonance imaging. J Neurosci Res 2003;73:284–95.
12. Daldrup-Link HE, Meier R, Rudelius M, Piontek G, Piert M, Metz S, Settles M, Uherek C, Wels W, Schlegel J, Rummeny EJ. In vivo tracking of genetically engineered, anti-HER2/neu directed natural killer cells to HER2/neu positive mammary tumors with magnetic resonance imaging. Eur Radiol 2005;15:4–13.
13. Hauger O, Frost EE, van Heeswijk R, Deminiere C, Xue R, Delmas Y, Combe C, Moonen CT, Grenier N, Bulte JW. MR evaluation of the glomerular homing of magnetically labeled mesenchymal stem cells in a rat model of nephropathy. Radiology 2006;238:200–10.
14. Magnitsky S, Watson DJ, Walton RM, Pickup S, Bulte JW, Wolfe JH, Poptani H. In vivo and ex vivo MRI detection of localized and disseminated neural stem cell grafts in the mouse brain. Neuroimage 2005;26:744–54.
15. Walter GA, Cahill KS, Huard J, Feng H, Douglas T, Sweeney HL, Bulte JW. Noninvasive monitoring of stem cell transfer for muscle disorders. Magn Reson Med 2004;51:273–7.
16. Metz S, Bonaterra G, Rudelius M, Settles M, Rummeny EJ, Daldrup-Link HE. Capacity of human monocytes to phagocytose approved iron oxide MR contrast agents in vitro. Eur Radiol 2004;14:1851–8.
17. Heyn C, Bowen CV, Rutt BK, Foster PJ. Detection threshold of single SPIO-labeled cells with FIESTA. Magn Reson Med 2005;53:312–20.
18. Bulte JW, Douglas T, Witwer B, Zhang SC, Strable E, Lewis BK, Zywicke H, Miller B, van Gelderen P, Moskowitz BM, Duncan ID, Frank JA. Magnetodendrimers allow endosomal magnetic labeling and in vivo tracking of stem cells. Nat Biotechnol 2001;19:1141–7.
19. Lewin M, Carlesso N, Tung CH, Tang XW, Cory D, Scadden DT, Weissleder R. Tat peptide-derivatized magnetic nanoparticles allow in vivo tracking and recovery of progenitor cells. Nat Biotechnol 2000;18:410–14.
20. Daldrup-Link HE, Rudelius M, Oostendorp RA, Jacobs VR, Simon GH, Gooding C, Rummeny EJ. Comparison of iron oxide labeling properties of hematopoietic progenitor cells from umbilical cord blood and from peripheral blood for subsequent in vivo tracking in a xenotransplant mouse model XXX. Acad Radiol 2005;12:502–10.
21. Daldrup-Link HE, Rudelius M, Piontek G, Metz S, Brauer R, Debus G, Corot C, Schlegel J, Link TM, Peschel C, Rummeny EJ, Oostendorp RA. Migration of iron oxide-labeled human hematopoietic progenitor cells in a mouse model: in vivo monitoring with 1.5-T MR imaging equipment. Radiology 2005;234:197–205.
22. Arbab AS, Yocum GT, Kalish H, Jordan EK, Anderson SA, Khakoo AY, Read EJ, Frank JA. Efficient magnetic cell labeling with protamine sulfate complexed to ferumoxides for cellular MRI. Blood 2004;104:1217–23.
23. Arbab AS, Bashaw LA, Miller BR, Jordan EK, Bulte JW, Frank JA. Intracytoplasmic tagging of cells with ferumoxides and transfection agent for cellular magnetic resonance imaging after cell transplantation: methods and techniques. Transplantation 2003;76:1123–30.
24. Arbab AS, Yocum GT, Rad AM, Khakoo AY, Fellowes V, Read EJ, Frank JA. Labeling of cells with ferumoxides-protamine sulfate complexes does not inhibit function or differentiation capacity of hematopoietic or mesenchymal stem cells. NMR Biomed 2005;18:553–9.
25. Weber A, Pedrosa I, Kawamoto A, Himes N, Munasinghe J, Asahara T, Rofsky NM, Losordo DW. Magnetic resonance mapping of transplanted endothelial progenitor cells for therapeutic neovascularization in ischemic heart disease. Eur J Cardiothorac Surg 2004;26:137–43.
26. Hoehn M, Kustermann E, Blunk J, Wiedermann D, Trapp T, Wecker S, Focking M, Arnold H, Hescheler J, Fleischmann BK, Schwindt W, Buhrle C. Monitoring of implanted stem cell migration in vivo: a highly resolved in vivo magnetic resonance imaging investigation of experimental stroke in rat. Proc Natl Acad Sci USA 2002;99:16267–72.
27. Stroh A, Faber C, Neuberger T, Lorenz P, Sieland K, Jakob PM, Webb A, Pilgrimm H, Schober R, Pohl EE, Zimmer C. In vivo detection limits of magnetically labeled embryonic stem cells in the rat brain using high-field (17.6 T) magnetic resonance imaging. Neuroimage 2005;24:635–45.
28. Heyn C, Ronald JA, Mackenzie LT, MacDonald IC, Chambers AF, Rutt BK, Foster PJ. In vivo magnetic resonance imaging of single cells in mouse brain with optical validation. Magn Reson Med 2006;55:23–9.
29. de Vries IJ, Lesterhuis WJ, Barentsz JO, Verdijk P, van Krieken JH, Boerman OC, Oyen WJ, Bonenkamp JJ, Boezeman JB, Adema GJ, Bulte JW, Scheenen TW, et al. Magnetic resonance tracking of dendritic cells in melanoma patients for monitoring of cellular therapy. Nat Biotechnol 2005;23:1407–13.
30. de Vries IJ, Eggert AA, Scharenborg NM, Vissers JL, Lesterhuis WJ, Boerman OC, Punt CJ, Adema GJ, Figdor CG. Phenotypical and functional characterization of clinical grade dendritic cells. J Immunother 2002;25:429–38.
31. Thurner B, Haendle I, Roder C, Dieckmann D, Keikavoussi P, Jonuleit H, Bender A, Maczek C, Schreiner D, von den DP, Brocker EB, Steinman RM, et al. Vaccination with mage-3A1 peptide-pulsed mature, monocyte-derived dendritic cells expands specific cytotoxic T cells and induces regression of some metastases in advanced stage IV melanoma. J Exp Med 1999;190:1669–78.
32. Bulte JW, Miller GF, Vymazal J, Brooks RA, Frank JA. Hepatic hemosiderosis in non-human primates: quantification of liver iron using different field strengths. Magn Reson Med 1997;37:530–6.
33. Bulte JW, Arbab AS, Douglas T, Frank JA. Preparation of magnetically labeled cells for cell tracking by magnetic resonance imaging. Methods Enzymol 2004;386:275–99.

34. Bakker AB, Schreurs MW, de Boer AJ, Kawakami Y, Rosenberg SA, Adema GJ, Figdor CG. Melanocyte lineage-specific antigen gp100 is recognized by melanoma-derived tumor-infiltrating lymphocytes. J Exp Med 1994;179:1005–9.
35. Krooshoop DJ, Torensma R, van den Bosch GJ, Nelissen JM, Figdor CG, Raymakers RA, Boezeman JB. An automated multi well cell track system to study leukocyte migration. J Immunol Methods 2003; 280:89–102.
36. de Vries IJ, Lesterhuis WJ, Scharenborg NM, Engelen LP, Ruiter DJ, Gerritsen MJ, Croockewit S, Britten CM, Torensma R, Adema GJ, Figdor CG, Punt CJ. Maturation of dendritic cells is a prerequisite for inducing immune responses in advanced melanoma patients. Clin Cancer Res 2003;9:5091–100.
37. Schultz JF, Bell JD, Goldstein RM, Kuhn JA, McCarty TM. Hepatic tumor imaging using iron oxide MRI: comparison with computed tomography, clinical impact, and cost analysis. Ann Surg Oncol 1999; 6:691–8.
38. Baumjohann D, Hess A, Budinsky L, Brune K, Schuler G, Lutz M. In vivo magnetic resonance imaging of dendritic cell migration into the draining lymph nodes of mice. Eur J Immunol 2006;211:587–97.
39. de Vries IJ, Bernsen MR, Lesterhuis WJ, Scharenborg NM, Strijk SP, Gerritsen MJ, Ruiter DJ, Figdor CG, Punt CJ, Adema GJ. Immunomonitoring tumor-specific T cells in delayed-type hypersensitivity skin biopsies after dendritic cell vaccination correlates with clinical outcome. J Clin Oncol 2005;23:5779–87.
40. Blocklet D, Toungouz M, Kiss R, Lambermont M, Velu T, Duriau D, Goldman M, Goldman S. ^{111}In-oxine and 99mTc-HMPAO labelling of antigen-loaded dendritic cells: in vivo imaging and influence on motility and actin content. Eur J Nucl Med Mol Imaging 2003;30: 440–7.
41. Eggert AA, Schreurs MW, Boerman OC, Oyen WJ, de Boer AJ, Punt CJ, Figdor CG, Adema GJ. Biodistribution and vaccine efficiency of murine dendritic cells are dependent on the route of administration. Cancer Res 1999;59:3340–5.